Journal of Structural Geology 33 (2011) 891–897

Contents lists available at ScienceDirect

Journal of Structural Geology

journal homepage: www.elsevier.com/locate/jsg

Nature and tectonic significance of co-seismic structures associated with the Mw 8.8 Maule earthquake, central-southern Chile forearc

C. Arriagada [a,*], G. Arancibia [b], J. Cembrano [b], F. Martínez [a], D. Carrizo [a], M. Van Sint Jan [b], E. Sáez [b], G. González [c], S. Rebolledo [a], S.A. Sepúlveda [a], E. Contreras-Reyes [d], E. Jensen [c], G. Yañez [b]

[a] Departamento de Geología-Centro de Excelencia en Geotermia de Los Andes (CEGA-FONDAP), Universidad de Chile, Plaza Ercilla 803, Santiago, Chile
[b] Departamento de Ingeniería Estructural y Geotécnica, Pontificia Universidad Católica de Chile, Avda. Vicuña Mackenna 4860, Santiago, Chile
[c] Departamento de Ciencias Geológicas, Universidad Católica del Norte, Avda. Angamos 0610, Antofagasta, Chile
[d] Departamento de Geofisica, Universidad de Chile, Blanco Encalada 2002, Santiago, Chile

ARTICLE INFO

Article history:
Received 13 June 2010
Received in revised form
28 January 2011
Accepted 2 March 2011
Available online 10 March 2011

Keywords:
co-seismic
Mw 8.8 Maule earthquake
central southern Chile forearc
active tectonics

ABSTRACT

The Mw 8.8 Maule earthquake on February 27, 2010 affected the central-southern Chilean forearc of the Central Andes. Here we show the results of field investigations of surface deformation associated with this major earthquake. Observations were carried out within three weeks after the seismic event, mostly in the central and northern part of the forearc overlying the rupture zone. We provide a detailed field record of co-seismic surface deformation and examine its implications on active Andean tectonics. Surface rupture consisted primarily of extensional cracks, push-up structures, fissures with minor lateral displacements and a few but impressive extensional geometries similar to those observed in analogical modeling of rift systems. A major group of NW-WNW striking fractures representing co-seismic extensional deformation is found at all localities. These appear to be spatially correlated to long-lived basement fault zones. The NW-striking normal focal mechanism of the Mw 6.9 aftershock occurred on March 11 demonstrates that the basement faults were reactivated by the Mw 8.8 Maule earthquake. The co-seismic surface ruptures show patterns of distributed deformation similar to those observed in mapped basement-involved structures. We propose that co-seismic reactivation of basement structures play a fundamental role in stress release in the upper plate during large subduction earthquakes. The fundamental mechanism that promotes stress relaxation is largely driven by elastic rebound of the upper plate located right above the main rupture zone.

1. Introduction

The Mw 8.8 Maule earthquake on the morning of February 27, 2010 was the largest seismic event of the Andes in the last 50 years (Fig. 1). It was an inter plate earthquake at the boundary between the overriding South American Plate and the subducting Nazca Plate. The quake generated a tsunami causing significant devastation along the south-central Chilean coast including the Juan Fernandez Islands, and it was recorded throughout the Pacific Ocean. The mainshock rupture began propagating at 06:35:15 GMT, at a depth of about 24.1 km, with epicenter on coordinates 35.95°S, 73.15°W. The Harvard centroid-moment tensor (Harvard CMT Project), solution indicates thrust faulting on a shallowly (18°) east-dipping plane striking N18°E. The last large earthquake in this region was 20 February 1835 (Darwin, 1851) with an estimated magnitude about 8.5 (Lomnitz, 1971; Beck et al., 1998).

The aftershock distribution provides a first-order indication of the mainshock rupture size and shows that it propagates toward both the NNE and SSW directions (Fig. 1; Harvard CMT Project). The aftershock distribution suggests a rupture length of ca. 550 km, which overlaps the northern end of the rupture zone associated with the great 1960 earthquake, of magnitude 9.5 (Plafker and Savage, 1970; Cifuentes, 1989) and the southern termination of the rupture zones corresponding to the Mw 8.2 1906 and Mw 7.8 1985 Valparaiso earthquakes (Barrientos, 1995). Harvard CMT aftershock focal mechanisms display mostly thrust faulting consistent with the mainshock. Slip distribution of the mainshock from space geodesy and broadband teleseismic data show that megathrust slip below the coastline did not propagate to the north of 34°S (Delouis et al., 2010; Lay et al., 2010; Tong et al., 2010). In agreement with slip models, significant vertical co-seismic displacement in coastal areas between 2.5 and −1 m occurred between 34° and 38°30'S (Farías et al., 2010).

* Corresponding author.
E-mail address: cearriag@cec.uchile.cl (C. Arriagada).

0191-8141/$ – see front matter © 2011 Elsevier Ltd. All rights reserved.
doi:10.1016/j.jsg.2011.03.004

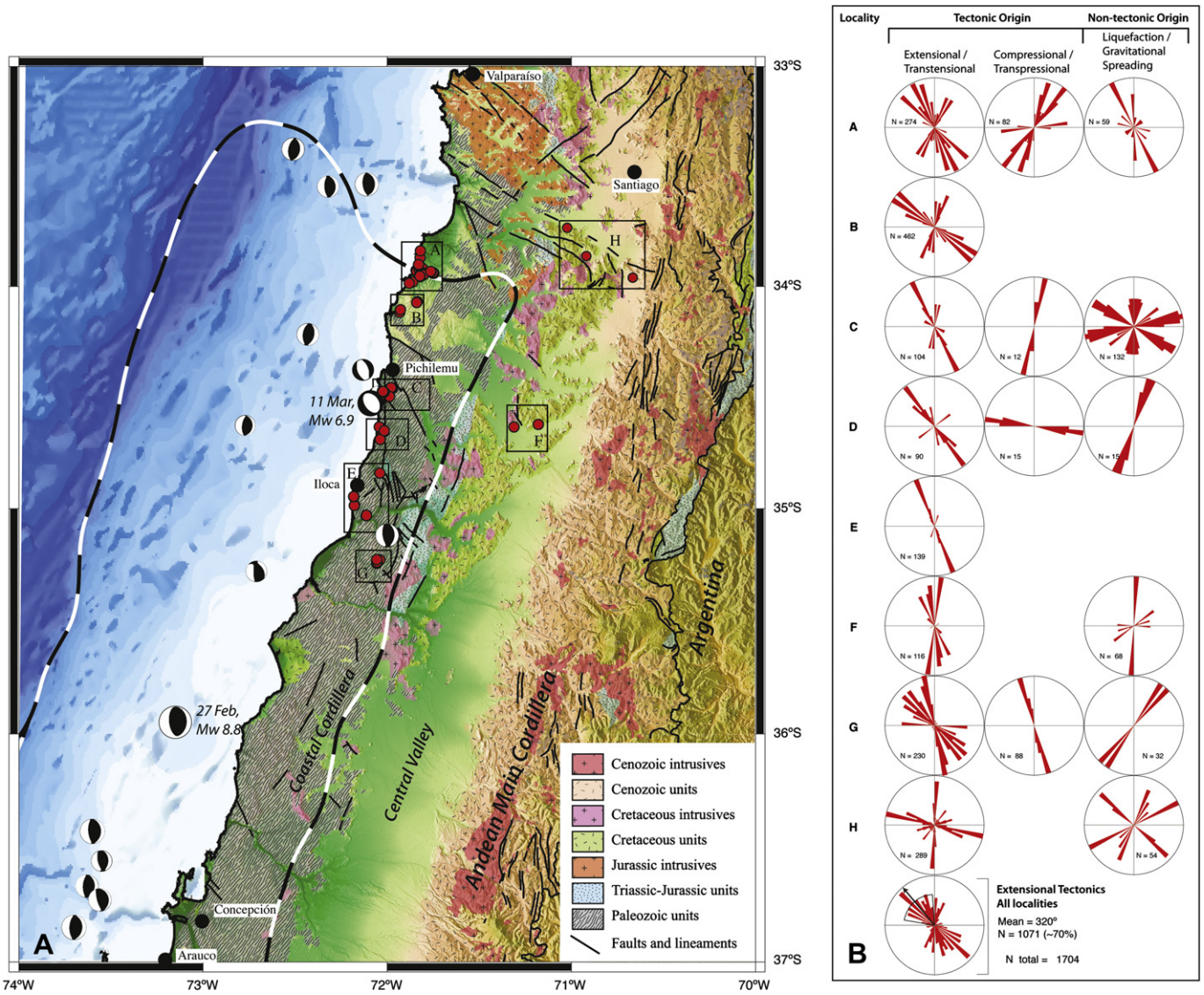

Fig. 1. A) Regional map showing earthquakes with magnitudes >5.0 from 27 February to 31 March 2010 (modified after Mapa Geológico (1:1000.000), SERNAGEOMIN Chile). Moment tensor solutions from the Harvard CMT catalog are shown for the 27 February mainshock (large solution) and aftershocks. Red dots show sites of measurements of co-seismic effects. The approximate co-seismic rupture zone of the 2010 Maule earthquake is showed with black and white color segmented line (modified after Delouis et al., 2010; Lay et al., 2010; Tong et al., 2010; Moreno et al., 2010). B) Rose diagrams showing the strike of mapped surface ruptures. The red color on rose diagrams for Extensional/Transtentional and Liquefaction/Gravitational Spreading (Compressional–Transpressional) represent extensional-transtensional cracks (fold axes, reverse faults and trends of push-up structures). (For interpretation of the references to colour in this figure legend, the reader is referred to the web version of this article).

A contrasting aftershock sequence was represented by a swarm of events close to Pichilemu in the northern segment of the mainshock rupture (Fig. 1). The swarm included a 6.9 magnitude earthquake followed by two 6.7–6.0 aftershocks that occurred on March 11. The focal mechanism indicates NW-striking normal faulting (Fig. 1; Harvard CMT Project). The hypocenters of this somehow puzzling aftershock sequence are concentrated at crustal levels within the continental lithosphere (Harvard CMT Project). During the following two-three weeks, tens of smaller aftershocks have been aligned with the same NW strike and SE propagation, delineating a well-defined rupture orientation.

Because much of the direct observation of the surface displacements produced by subduction earthquakes is submarine, and commonly limited, analyses of the nature and significance of co-seismic surface ruptures are very scarce (Plafker, 1965; Collot et al., 2004; Contreras-Reyes et al., 2010). One of the most remarkable examples, where significant forearc deformation related to upper plate faulting occurred during the Mw 9.2 1964 Alaska earthquake (Plafker, 1965). Critical information concerning seismic faulting mechanics and seismic hazards, as well as the crustal deformation modes of the continental crust and long-term nature of great earthquakes can be unraveled from the description and interpretation of co-seismic deformation. Meter-scale cracks, formed during and/or shortly after strong subduction earthquakes, have been used to map characteristic ruptures in the hyperarid climate of coastal areas in northern Chile and southern Peru (Loveless et al., 2009; 2010).

During the 2010 mainshock, widespread co-seismic surface ruptures formed in the outer forearc region, on top of the rupture area. Field data were collected during the first weeks after the mainshock, when most co-seismic structures were still well preserved. For the sake of efficiency, we simultaneously deployed three teams, each focusing on different areas. Here, we present the nature, geometry and kinematics of the co-seismic surface ruptures

produced in the northern part of the area affected by the mainshock with the aim of provide insights into the effects of a large subduction inter plate earthquake on the nature and extent of surface deformation. From this, in turn, we can better understand the way by which stresses are transferred to the upper plate during and after a large earthquake.

2. Tectonic setting

The Nazca-South American plate boundary runs for several thousand km from the triple junction of the Nazca, South American, and Antarctic plates at 46°S latitude to northwestern South America. Plate convergence takes place at ca. 70 mm/year in a N78°E direction (Angermann et al., 1999). The Andean segment corresponding to the rupture area of the Mw 8.8 2010 earthquake extends approximately from south of Valparaiso to the Arauco Península (Fig. 1). In this segment, the Central Andes exhibit modest Cenozoic shortening in comparison with the northernmost part of this Cordillera (e.g. Ramos et al., 2004). Remarkably, the northern and southern ends of the rupture zone coincide very well with changes in trench orientation, suggesting long-term geologic controls of subduction earthquakes in the Andean margin (e.g. Allmendinger et al., 2010; Cembrano et al., 2010) (Fig. 1).

The main regional-scale structures of the Coastal Cordillera segment are a series of WNW and NW-striking, subvertical fault zones that run across the continental margin (Fig. 1). The precise

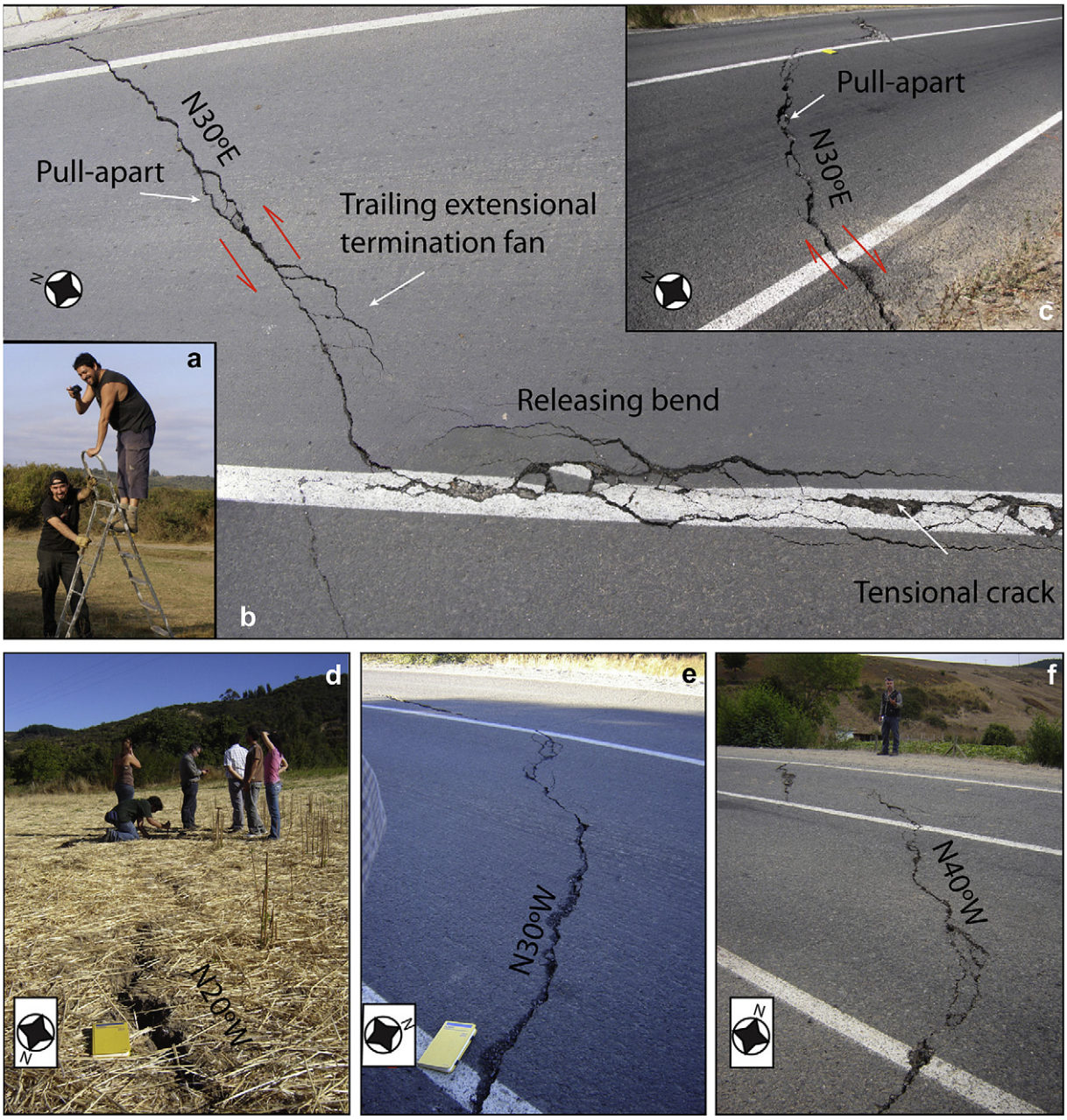

Fig. 2. Representative photographs of co-seismic open cracks without significant vertical displacements. (a) During the field trip a stepladder was used to obtain nearly orthogonal to the surface images in order to map the main structural features; (b) Main structural features draped over a nearly orthogonal photograph showing co-seismic NE-SW left-lateral and normal displacement in locality A. (c) Evidence for NE-SW right lateral and normal displacement in locality A. (d) N 20°W extensional cracks in locality A. (e) Evidence for NW-SE extensional cracks with left-lateral displacement in locality A. (f) NW-SE extensional cracks in locality D.

nature and timing of displacement along these fault zones is poorly known, although they have been interpreted as long-lived basement structures reactivated at different times, at least from the Mesozoic (e.g. Wall et al., 1996; Yañez et al., 1998; Rivera and Cembrano, 2000; Rivera and Yáñez, 2009). Recent studies suggest that some of these faults may be active today and thus represent seismic hazard (e.g. Sabaj et al., 2010).

3. Co-seismic, surface ruptures

We recognized co-seismic surface ruptures at 52 different sites distributed throughout the northern part of the area affected by the mainshock (Fig. 1). We organized the sites into 8 localities according to their spatial distribution. Localities (A–E) are distributed along the western edge of the Coastal Cordillera. Localities (F–G) are in the inner part of the Coastal Cordillera and locality (H) lies at the eastern edge of the Coastal Cordillera, immediately south of Santiago, Chile's capital (Fig. 1).

During the field work we had the opportunity to interview numerous inhabitants of the region affected by the earthquake. According to information provided by residents, the observed ruptures occurred during the mainshock. Furthermore, some of the authors of this paper were mapping co-seismic surface ruptures in the field close to the epicenter of the Mw 6.9 aftershock that occurred in March 11 at Pichilemu. There they could observe that no new cracks formed during this aftershock and that previously formed cracks were not affected.

Field observations were conducted along road sections and accessible footpaths, along and across the valleys. Direct observation of the structures was conducted with the aid of a stepladder to produce local detailed maps (Fig. 2a). Co-seismic fractures were weighed according to their length, to avoid over-representation of short fractures (1 m or less) or under-representation of long ones (several meters). Thus, for internal consistency, each individual fracture was represented in the rose diagram by the number of 1 m long segments forming its entire length.

We have identified two main fracture types according to their geometry and kinematics regardless of their origin, which are addressed separately: (1) Extensional-transtensional, and (2) Compressional-transpressional.

3.1. Extensional-transtensional fractures

Extensional-transtensional cracks are widely distributed in the visited localities and consist of several segments of cracks trending NNW-WNW and NNE-ENE that affect soft rocks, fluvial/alluvial deposits, soils and paved/dirt roads (Figs. 1–3).

When possible, we differentiated cracks triggered by liquefaction or by mass wasting (non-tectonic origin) from others more likely produced by static stress fields generated during the mainshock (tectonic origin) (Fig. 1, see supplementary material Table S1).

Randomly-striking cracks systematically occur on fluvial deposits in the vicinity of small creeks and rivers, where they strike sub-parallel to the local stream direction. These cracks may exhibit a surrounding zone covered with well-sorted sand deposits that appear to have been ejected from the fractures, which are then interpreted as triggered by liquefaction (Fig. 3a). Similarly, ground deformation associated with open cracks/faults on hill slopes and unconfined road stretches appear to be the result of local mass wasting (flows and lateral and gravitational spreading) (Fig. 3b–c).

Fig. 3. Photographs showing extensional-transtensional co-seismic fractures. (a) sand boils caused by liquefaction in locality G. (b) extensional cracks caused by liquefaction in locality C. (c) extensional cracks caused by landslide in the Ruta 5 highway (locality H). (d & e) EW-striking open fissures, up to 1.5 m wide and up to 50 cm deep, in a soccer field in San Antonio de Naltahua town (locality H). (f) NNW-striking ruptures in locality E close to the village of Iloca. (g) NNW-striking fissures (up to 50 cm wide and 30 cm deep) in locality B. (h & i) ENE-EW-striking co-seismic structural features giving the appearance of a symmetrical graben which are very similar to those described in analog models.

Most of the surface ruptures which we interpret to represent stress fields occur with consistent trends cross-cutting hill ridges, fluvial terraces and paved and unpaved roads (Figs. 2 and 3). The surface cracks are defined by numerous, adjacent segments of interlinked extensional and/or shear fractures (Figs. 2 and 3). Detailed mapping of the ruptures show that most of them are in the range of 10–100 m-long by 5–15 cm wide. Several centimeter-to-meter long segments making up the main cracks may locally show curved shapes, zig–zag patterns, step-overs and variable components of bulk sinistral and dextral horizontal separation (Fig. 2). Both left and right lateral strike- slip offset was observed at some locations along the surface zone especially in paved roads, and range from less than 1 cm to 3 cm (Fig. 2b–f). Co-seismic, NW-striking surface ruptures were recognized in all localities and represent the most persistent orientation (~70%, Fig. 1). A minor proportion (~30%) of cracks strike NNE and NS.

The most prominent co-seismic fractures were observed in localities B, C, E and H (Fig. 3d–i). A remarkable case occurred at locality H. There, ~EW-striking graben structures affect a soccer field and several houses, and can be followed along-strike for more than 5 km (Fig. 3e). This graben structure is probably tectonic in origin because no evidence for liquefaction and/or gravitational spreading was found (Supplementary material Figure S1).

Individual NNW-striking ruptures reach 60 m long on top of a cliff east of Iloca (Fig. 3f), which can be interpreted as the result of tectonic extension while structures dip both in favor and against the local slope, ruling out a mass wasting origin.

At least 500 m-long surface ruptures occurred in locality C close to the coast and parallel to the northern shore of a local lagoon. Here a series of symmetrical rift zones occurred, similar to those observed in analog models of extensional tectonics (Fig. 3h). In spite of these observations, we cannot entirely rule out that these fractures were induced by liquefaction because of their shore-parallel orientation and proximity to a water body.

Co-seismic displacements were locally measured along the surface rupture zone based on offset linear surface-markers such as roads. The maximum opening of these cracks is about 10 cm, maximum horizontal displacement up to 5 cm, whereas the vertical displacements range generally between 1 and 20 cm (Figs. 2 and 3). On site H, vertical displacements range from less than 1 cm to up to 60 cm in the central part of the soccer field (Fig. 3d,e).

3.2. Compressional-transpressional features

Fold-and-thrust structures, including mole tracks are also seen on some observation sites, generally developed within alluvial deposits, dirt roads and sidewalks (Figs. 1,4 and 5). Compressional co-seismic features were found in localities A, C and E (Fig. 1). The mole tracks are typically 2–30 cm in height, 0.2–1 m in width and 1–15 m in length (Figs. 4 and 5). The axis of the mole tracks strikes mainly NNE-SSW to NE-SW in localities A and C, and frequently trend fairly orthogonal, but not completely, to the overall trend of adjacent, coeval, extensional fractures zones (Figs. 1–4). For instance, at one site in locality E the axes of angular-ridge type mole tracks observed in sidewalks are following a similar orientation to the NNW-striking extensional tectonic cracks (Figs. 1–5d–f).

The mole track structures that formed within the co-seismic surface in localities A and C are considered to represent contractional

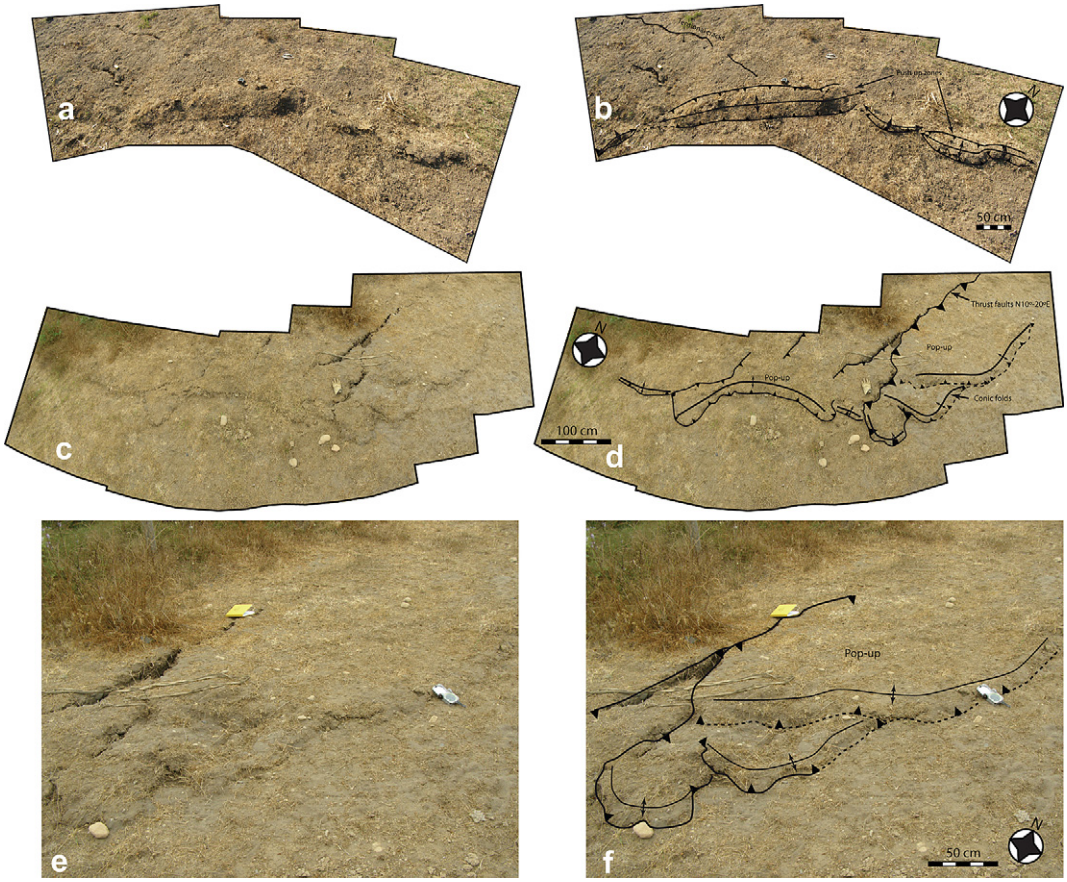

Fig. 4. Co-seismic fold-and-thrust structures developed in locality A. (a–b) & (c–d) Map view of NNE- to EW-trending folds and related reverse faults with opposite vergence developing pop-up structures. (e–f) Detail of photograph c & d, vertical uplift of the surface rupture is up to 5 cm.

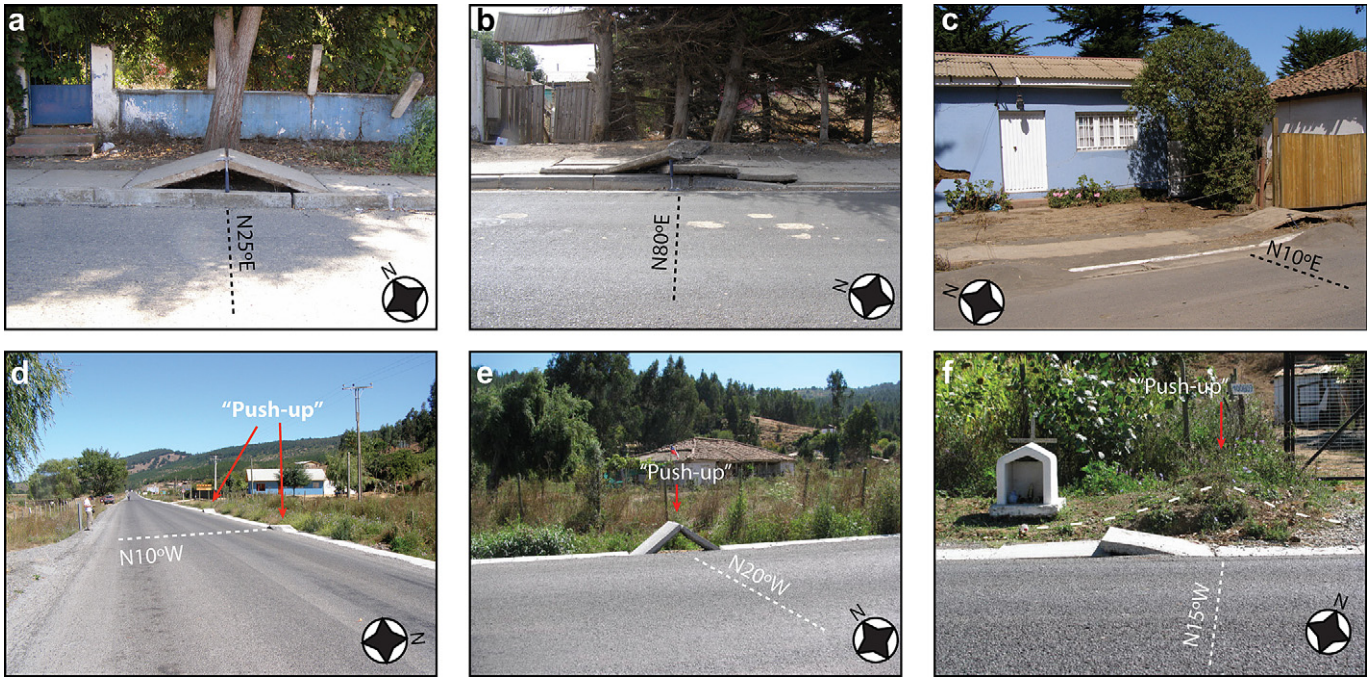

Fig. 5. Typical co-seismic angular-ridge type mole track structures developed within sealed roads at different localities. (a–b) Locality A (c) Locality C (d–f) Locality E.

structures associated with thrusting and folding. Parallelism between extensional and contractional structures observed in locality E of the area suggests that some structures can be related to dynamic stress modulated by seismic wave propagation.

4. Discussion

The pattern of co-seismic surface displacements can be reproduced by elastic dislocation models of the mainshock rupture (e.g. Chlieh et al., 2004; Loveless et al., 2009). However, extensive transtensional-extensional and transpressional-compressional structures observed along the forearc overlying the main rupture zone produced by the 2010 Mw 8.8 Maule earthquake show that the local and regional patterns of surface deformation is significantly more complex than those predicted by simple elastic models. Detailed mapping reveals that the mainshock produced a permanent surface deformation in the outer forearc characterized by predominantly NW-WNW (~70%) and subordinated (~30%) NE-SW-striking extensional cracks (Localities A, B, C, D, E & G) and NE-SSW-trending compressional co-seismic features. Overall, there is a good agreement between the observed strikes of NW and WNW striking extensional cracks from localities A, B and H and the NE-SW-directed co-seismic horizontal displacement observed and computed from GPS near Valparaiso and Santiago (Delouis et al., 2010; Allmendinger et al., 2010).

A close spatial match occurs between the NW-WNW striking co-seismic surface ruptures and the NW-striking normal faulting aftershocks events that started on March 11th (Fig. 1). The zone of co-seismic NNW-NW surface structures, 200 km long and 30–50 km wide, seems to be spatially associated with pre-existing NW-WNW faults (Fig. 1). These were partially reactivated as extensional faults during the mainshock implying that co-seismic deformation and local ground ruptures during major inter plate earthquakes can be, at least in part, controlled by inherited, apparently inactive, long-term structures, producing trench-oblique forearc extension. NE-SW extension and NW-SE shortening characterizes the forearc overlying the northern tip of the main rupture.

Activity of these oblique to the Andes structures seems to be a first-order control on continental plate deformation style during the co-seismic period of large earthquakes (e.g. Allmendinger et al., 2010; Cembrano et al., 2010). In northern Chile, long-term, trench-orthogonal, forearc extension has been widely documented (e.g. González et al., 2003; Loveless et al., 2009). There, a complex system of Pliocene-Pleistocene open cracks and sub-parallel normal faults has been interpreted alternatively as the result of (1) co-seismic elastic rebound during large subduction earthquakes (e.g. Delouis et al., 1998; González et al. 2003; Allmendinger and González, 2009); (2) Regional uplift followed by gravitational collapse (e.g. Niemeyer et al. 1996); and/or (3) interseismic warping of the forearc surface (Loveless et al., 2009). In the latter case, extension would take place locally at the hinge zone of long wavelength folds.

In our case, in turn, it is obvious that all studied fractures are co-seismic. In the studied area, most of co-seismic deformation can be explained by elastic rebound of the upper plate and locally by liquefaction phenomena and gravitational landslides. Elastic rebound would produce an ENE-trending extension direction sub-parallel to the convergence vector, i.e orthogonal to the predominant NNW-strike of the co-seismic extensional/transtensional fractures. The aftershock sequence, although kinematically compatible with the described co-seismic cracks, did not produce new surface cracks and so all the observed deformation can be attributed to the mainshock.

Thus, one of the main implications of our field observations is that the co-seismic reactivation of NW-WNW, long-lived basement structures should be considered in subsequent slip models of the surface deformation associated with the Maule earthquake.

5. Conclusions

Based on the results of field observations localized right above of the northern tip of the main rupture following the Mw 8.8, 2010

Maule earthquake, we arrived at the following conclusions regarding co-seismic surface deformation produced during the earthquake:

1. Co-seismic ruptures were widely developed and consisted primarily of extensional cracks, push-up structures, fissures with minor lateral displacements and a few but impressive geometries similar to those observed in analogical modeling of rift systems.
2. Most of co-seismic deformation can be explained by elastic rebound of the upper plate and locally by liquefaction phenomena and gravitational landslides.
3. NW-striking extensional co-seismic ruptures were recognized in all localities, represent the most persistent orientation and seem to be spatially associated with pre-existing NW-WNW faults that were partially reactivated as extensional faults during the mainshock.
4. Our results suggest that co-seismic deformation and local ground ruptures during major inter plate earthquakes can be, at least in part, controlled by inherited, apparently inactive, long-lived structures.
5. Thus, long-lived basement structures should be considered in subsequent slip models of the surface deformation associated with the Maule earthquake.

Acknowledgements

We acknowledge support by the Engineering and Geotechnical Department, Universidad Católica de Chile, the Departamento de Geología and Departamento de Geofísica at the Universidad de Chile and the Departamento de Ciencias Geológicas de la Universidad Católica del Norte. Discussions with Rick Allmendinger and Orlando Rivera are greatly appreciated. We thank editor Cees W. Passchier, Kate Clark and an anonymous referee for detailed, thoughtful reviews that improved the manuscript.

Appendix. Supplementary material

Supplementary data associated with this article can be found in the online version, at doi:10.1016/j.jsg.2011.03.004.

References

Allmendinger, R.W., González, G., 2009. Neogene to Quaternary tectonics of the 237 coastal Cordillera, northern Chile. Tectonophysics. doi:10.1016/j.tecto.2009.04.019.

Allmendinger, R.W., Yáñez, G., Cembrano, J., 2010. Interseismic strain, continental deformation, and great earthquakes of southern Chile. Abstract presented at the AGU Chapman Conference on Giant earthquakes and their tsunamis. Valparaíso, Chile.

Angermann, D., Klotz, J., Reigber, C., 1999. Space-geodetic estimation of the Nazca-South America Euler vector. Earth Planet. Sci. Lett. 171, 329–334.

Barrientos, S.E., 1995. Dual seismogenic behavior: the 1985 Central Chile earthquake. Geophys. Res. Lett. 22, 3541–3544.

Beck, S., Barrientos, S., Kausel, E., Reyes, M., 1998. Source characteristics of historic earthquakes along the central Chile subduction zone. J. South. Am. Earth Sci. 11, 115–129.

Cembrano, J., Yañez, G., Allmendinger, R.W., González, G., Rivera, O., Arancibia, G., 2010. Long-term geological controls on the nature and extension of earthquake rupture zones in the Chilean Andes: lessons from the 2010, Mw 8.8 Maule Earthquake. Gordon Conference on Rock Deformation, Tilton, NH, USA.

Chlieh, M., de Chabalier, J.B., Ruegg, J.C., Armijo, R., Dmowska, R., Campos, J., Feigl, K.L., 2004. Crustal deformation and fault slip during the seismic cycle in the North Chile subduction zone, from GPS and InSAR observations. Geophys. J. Int. 158, 695–711.

Cifuentes, I.L., 1989. The 1960 Chilean earthquake. J. Geophys. Res. 94, 665–680.

Collot, J.-Y., Marcaillou, B., Sage, F., Michaud, F., Agudelo, W., Charvis, P., Graindorge, D., Gutscher, M.A., Spence, G.D., 2004. Are rupture zone limits of great subduction earthquakes controlled by upper plate structures? Evidence from multichannel seismic reflection data acquired across the N-Ecuador-SW Colombia margin. J. Geophys. Res. 109. doi:10.1029/2004JB003060.

Contreras-Reyes, E., Flueh, E.R., Grevemeyer, I., 2010. Tectonic control on sediment accretion and subduction of south central Chile: Implications for coseismic rupture processes of the 1960 and 2010 megathrust earthquakes. Tectonics 29, TC6018. doi:10.1029/2010TC002734.

Darwin, C., 1851. Geological Observations on Coral Reefs, Volcanic Islands and on South America. Smith, Elder and Co, Londres. 768p.

Delouis, B., Philip, H., Dorbath, L., Cisternas, A., 1998. Recent crustal deformation in the Antofagasta region (northern Chile) and the subduction process. Geophys. J. Int. 132, 302–338.

Delouis, B., Nocquet, J.-M., Vallée, M., 2010. Slip distribution of the February 27, 2010 Mw = 8.8 Maule Earthquake, central Chile, from static and high-rate GPS, InSAR, and broadband teleseismic data. Geophys. Res. Lett. 37, L17305. doi:10.1029/2010GL043899.

Farías, M., Vargas, G., Tassara, A., Carretier, S., Baize, S., Melnick, D., Bataille, K., 2010. Land-Level changes produced by the M_w 8.8 2010 Chilean earthquake. Science 329 (5994), 916. doi:10.1126/science.1192094.

González, G., Cembrano, J., Carrizo, D., Macci, A., Schneider, H., 2003. Link between 262 forearc tectonics and Pliocene-Quaternary deformation of the coastal Cordillera, northern Chile. J. South Am. Earth Sci. 18, 321–342.

Harvard CMT Project, see http://www.globalcmt.org/CMTsearch.html.

Lay, T., Ammon, C.J., Kanamori, H., Koper, K.D., Sufri, O., Hutko, A.R., 2010. Teleseismic inversion for rupture process of the 27 February 2010 Chile (M_w 8.8) earthquake. Geophys. Res. Lett. 37, L13301. doi:10.1029/2010GL043379.

Lomnitz, C., 1971. Grandes terremotos y tsunamis en Chile durante el periodo 1535–1955. Geofis. Panamericana 1, 151–178.

Loveless, J.P., Allmendinger, R., Pritchard, M., Garroway, J., González, G., 2009. Surface cracks record long-term seismic segmentation of the Andean margin. Geology 37, 23–26.

Loveless, J.P., Allmendinger, R.W., Pritchard, M.E., González, G., 2010. Normal and reverse faulting driven by the subduction zone earthquake cycle in the northern Chilean forearc. Tectonics 29, TC2001. doi:10.1029/2009TC002465 http://www.agu.org/journals/ABS/2010/2009TC002465.shtml.

Moreno, M., Rosenau, M., Oncken, O., 2010. 2010 Maule earthquake slip correlates with pre-seismic locking of Andean subduction zone. Nature 467, 198–202. doi:10.1038/nature09349.

Niemeyer, H., González, G., Martinez-De Los Rios, E., 1996. Evolución tectónica cenozoica del margen continental activo de Antofagasta, norte de Chile. Revista Geológica de Chile 23, 165–186.

Plafker, G., 1965. Tectonic deformation associated with the 1964 Alaska earthquake. Science, v. 148, 1675–1687.

Plafker, G., Savage, J.C., 1970. Mechanism of the Chilean earthquake of may 21 and 22 1960. Geol. Soc. Am. Bull. 81, 1001–1030.

Ramos, V., Zapara, T., Cristallini, E., Introcaso, A., 2004. The Andean thrust system—latitudinal variations in structural styles and orogenic shortening. In: McClay, K.R. (Ed.), Thrust Tectonics and Hydrocarbons Systems: AAPG Memoir 82, 9, pp. 30–50.

Rivera, O.M. Cembrano, J. 2000. Modelo de formación de cuencas volcano-tectónicas en zonas de transferencia oblicuas a la cadena andina: el caso de las cuencas Oligo-Miocenas de Chile Central y su relación con estructuras WNW-NW (33°00–34°30'S). In Congreso Geológico Chileno, No. 9, Actas, vol. 2, p. 631–636. Puerto Varas.

Rivera, O., Yáñez, G., 2009. Naturaleza y Rol de Estructuras Translitosféricas en la Evolución del Arco Volcánico Oligo-Mioceno de Chile Central entre los 32° y 34° S. In: XII Congreso Geológico Chileno. Simposio S9 Tectónica Y Deformación Cortical Andina. Actas S9_092, Santiago, Chile. 5p.

Sabaj, R., Rebolledo, S., Leyton, F., Sepúlveda, S.A. 2010. Peligro sísmico asociado a las fallas potencialmente activas en la cordillera de la costa entre los 33° y 33,45°S. In: X Congreso Chileno de Sismología e Ingeniería Antisísmica, Valdivia-Santiago, Chile.

Tong, X., et al., 2010. The 2010 Maule, Chile earthquake: downdip rupture limit revealed by space geodesy. Geophys. Res. Lett. 37, L24311. doi:10.1029/2010GL045805.

Wall, R., Gana, P., Gutiérrez, A. 1996. Mapa geológico del área de San Antonio-Melipilla, regiones de Valparaíso, Metropolitana y del Libertador General Bernardo O'Higgins. In: Servicio Nacional de Geología y Minería, Mapas Geológicos, No. 2, 20 p., 1 mapa 1:100.000. Santiago.

Yañez, G., Gana, P., Fernández, R., 1998. Sobre el orígen y significado geológico de la anomalía Melipilla, zona central de Chile. Revista Geológica de Chile 25 (2), 175–198.